Virology **281,** 88–101 (2001)
doi:10.1006/viro.2000.0769, available online at http://www.idealibrary.com on IDEAL®

# Detection and Subcellular Localization of the Turnip Yellow Mosaic Virus 66K Replication Protein in Infected Cells

Delphine Prod'homme,* Sophie Le Panse,† Gabrièle Drugeon,* and Isabelle Jupin*,[1]

**Laboratoire de Virologie Moléculaire and †Service Commun de Microscopie Electronique, Institut Jacques Monod, UMR 7592, CNRS, Universités Paris 6–Paris 7, 2 place Jussieu, 75251 Paris Cedex 05, France*

*Received October 4, 2000; returned to author for revision October 27, 2000; accepted November 30, 2000*

Turnip yellow mosaic virus (TYMV) encodes a 206-kDa (206K) polyprotein with domains of methyltransferase, proteinase, NTPase/helicase, and RNA-dependent RNA polymerase (RdRp). *In vitro,* the 206K protein has been shown to undergo proteolytic processing, giving rise to the synthesis of 140-kDa (140K) and 66-kDa (66K) proteins, the latter comprising the RdRp protein domain. Antibodies were raised against the 66K protein and were used to detect the corresponding viral protein in infected cells; both leaf tissues and protoplasts were examined. The antiserum specifically recognized a protein of ~66 kDa, indicating that the cleavage observed *in vitro* is also functional *in vivo.* The 66K protein accumulates transiently during protoplast infection and localizes to cellular membrane fractions. Indirect immunoflorescence assays and electron microscopy of immunogold-decorated ultrathin sections of infected leaf tissue using anti-66K-specific antibody revealed labeling of membrane vesicles located at the chloroplast envelope. 

*Key Words:* viral replication; RdRp; transient accumulation; membrane vesicles; chloroplast envelope.

## INTRODUCTION

Turnip yellow mosaic virus (TYMV), the type member of the tymovirus group, is a small spherical plant virus that infects members of the Cruciferae (Matthews, 1973). TYMV possesses a monopartite positive-strand RNA genome, 6318 nucleotides long, that directs the expression of two extensively overlapping nonstructural proteins of 69 and 206 kDa (Morch *et al.,* 1988; Weiland and Dreher, 1989). A third ORF encodes the 20-kDa coat protein (CP), which is expressed from a subgenomic RNA (Pleij *et al.,* 1976).

The longer 206-kDa (206K) protein shows considerable amino acid sequence similarities with nonstructural putative replication proteins of several positive-strand RNA viruses. These data unequivocally linked tymoviruses with the "alpha-like" supergroup of viruses, which also comprises Sindbis virus (Goldbach and Wellink, 1988). The 206K protein has been shown to be necessary for TYMV RNA replication (Weiland and Dreher, 1989) and based on sequence comparisons, multiple domains indicative of methyltransferase, NTPase/helicase, and RNA-dependent RNA polymerase (RdRp) activities have been highlighted in the 206K protein (Morch *et al.,* 1988; Rozanov *et al.,* 1992; Gorbalenya *et al.,* 1989; Kamer and Argos, 1984). This large nonstructural protein also contains a papain-like cysteine proteinase domain located between the methyltransferase and the NTPase/helicase domains (Bransom and Dreher, 1994; Rozanov *et al.,* 1995). *In vitro* translation experiments have demonstrated that the 206K protein undergoes a cotranslational proteolytic cleavage (Morch *et al.,* 1989; Bransom *et al.,* 1991), giving rise to two protein products of 140 kDa (140K) and 66 kDa (66K). The N-terminus of the 140K protein is identical to the one of the 206K protein (Bénicourt and Haenni, 1978) and mapping of the cleavage site (Kadaré *et al.,* 1995; Bransom *et al.,* 1996) revealed that the resulting 140K protein carries the methyltransferase, proteinase, and NTPase/helicase motifs while the C-terminal 66K protein contains the RdRp domain. Both of these viral proteins are essential for the replication of the TYMV RNA genome (Weiland and Dreher, 1993). However, since the corresponding protein products have not yet been detected *in planta,* the mode of TYMV genome expression *in vivo* remains poorly understood. Likewise, little information is available on the temporal accumulation and subcellular localization of these proteins in infected plants. In addition, previously purified TYMV replicase fractions were shown to contain a 115-kDa protein of viral origin that is likely to arise from the processing of the 206K protein (Mouchès *et al.,* 1984; Candresse *et al.,* 1986), but whose origin is still unclear. In this study, we have prepared a potent antiserum to the TYMV 66K protein and have used it to detect the corresponding viral protein in infected cells, examining both leaf tissue and protoplasts. These antibodies specifically recognized a protein of molecular mass ~66 kDa, indi-

[1] To whom correspondence and reprint requests should be addressed. E-mail: jupin@ccr.jussieu.fr.

0042-6822/01 $35.00

cating that the cleavage observed *in vitro* also takes place *in vivo.* We found that the TYMV 66K protein accumulates transiently during viral infection and localizes to virus-induced membrane vesicles that are present at the chloroplast envelope. These data are consistent with previous observations (Laflèche and Bové, 1969; Laflèche *et al.,* 1972; Garnier *et al.,* 1986), suggesting that replication complexes of TYMV are associated with the chloroplast envelope.

## RESULTS

### Production of antibodies against the TYMV 66K protein

To produce a polyclonal antibody against the TYMV 66K protein, rabbits were immunized with purified His-66K protein, a recombinant protein expressed in insect cells via a baculovirus system (Héricourt *et al.,* 2000). This resulted in the production of an antiserum that strongly recognized the homologous immunogen on immunoblots and was able to immunoprecipitate the 66K protein produced in the rabbit reticulocyte *in vitro* translation system (Fig. 2, lane 5). This antibody will be referred to as anti-66K. Because these preliminary experiments revealed that the antiserum also cross-reacted with a compound present in the SDS–PAGE loading buffer (data not shown), the antiserum was first preadsorbed to minimize this background signal. The resulting preadsorbed antiserum was then tested in further immunoblot analysis for its capacity to detect viral-specific proteins in TYMV-infected Chinese cabbage and *Arabidopsis thaliana* protein extracts.

### Immunodetection of 66K protein and CP in TYMV-infected plants

Immunological analysis of TYMV-infected *A. thaliana* and Chinese cabbage plants was performed by Western blotting of leaf tissue extracts using the anti-66K antibodies (Fig. 1A). The major immunoreactive protein had an apparent molecular mass of approximately 66 kDa (lanes 2 and 3) and was absent from extracts of uninfected plants (lanes 1 and 4). No significant cross-reaction with host proteins was visible on the blot, but a set of fainter bands of lower molecular masses was also visible in the protein extracts from infected plants that may correspond to degradation products of the major 66K protein. No products of higher molecular mass could be detected. These data provide the first evidence that processing of the 206K protein to generate a polypeptide encompassing the RdRp domain is occurring *in planta.* The anti-CP antibody, used as a control, reacted specifically with the 20-kDa TYMV structural protein, in both infected *Arabidopsis* and Chinese cabbage plant extracts (Fig. 1B, lanes 2 and 3), while healthy tissues exhibited no significant labeling (lanes 1 and 4).

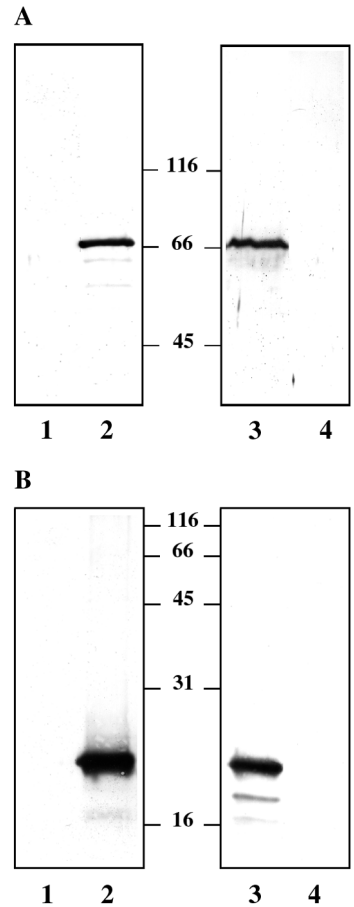


FIG. 1. Immunodetection of the TYMV 66K protein and CP in infected plants. Total proteins from healthy (lane 1) and TYMV-infected (lane 2) Chinese cabbage leaves, TYMV-infected (lane 3), and healthy (lane 4) *Arabidopsis* leaves were analyzed by SDS–PAGE on 7 (A) or 15% (B) polyacrylamide gels. The gels were electroblotted onto a nitrocellulose filter and proteins were revealed by Western blotting using the anti-66K (A) or the anti-CP (B) antisera. The position of molecular weight markers [$\beta$-galactosidase (116K), BSA (66K), ovalbumin (45K), carbonic anhydrase (31K) and myoglobin (16K)] is indicated.

To assess the electrophoretic mobility of the ~66-kDa protein detected *in planta,* compared to that of the *in vitro* cleavage products, extracts from TYMV-infected Chinese cabbage were loaded in parallel to $^{35}$S-labeled proteins obtained through *in vitro* translation of TYMV RNA or of a transcript encoding the 66K protein (Fig. 2). After transfer to nitrocellulose, the viral proteins were revealed both by Western blotting with the anti-66K antiserum (lanes 1–4) and by autoradiography (lanes 2′–4′). Because of their similar gel mobility and antibody recognition, we therefore assume that the species detected in infected plants is similar to the 66K protein observed *in vitro,* which corresponds to the C-terminal cleavage product of the 206K protein (Morch *et al.,* 1989; Bransom *et al.,* 1991). The viral protein detected in this study will therefore be referred to as TYMV 66K protein, in accordance with

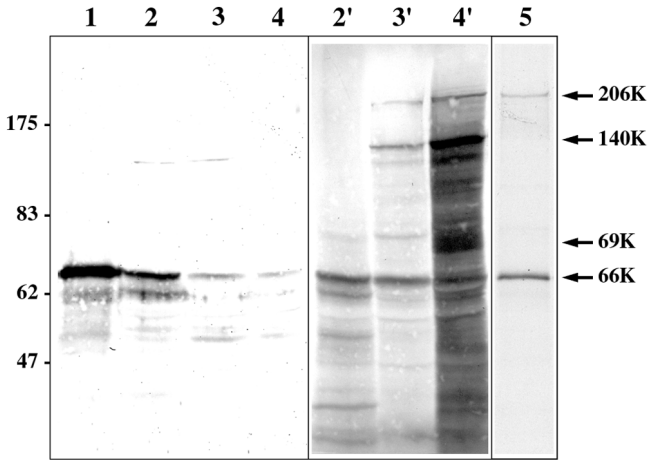


FIG. 2. The electrophoretic mobility of the 66-kDa protein detected *in planta* is similar to the 66K protein translated *in vitro*. Total proteins from TYMV-infected Chinese cabbage leaves (lane 1) and $^{35}$S-labeled proteins obtained through *in vitro* translation of T7-66K transcripts (lanes 2 and 2′) and TYMV RNA (lanes 3, 4, 3′, and 4′) were loaded in parallel lanes of the same gel. The proteins were separated by SDS–PAGE on a 7% polyacrylamide gel, electroblotted onto a nitrocellulose filter, and revealed both by Western blotting using the anti-66K antiserum (lanes 1 to 4) and by autoradiography (lanes 2′ to 4′). The position of prestained molecular weight markers (Biolabs) is indicated. Lanes 4 and 4′ correspond to standard *in vitro* translation conditions and the major labeled products synthesized by TYMV RNA [206K, 140K, 69K (apparent molecular mass 75 kDa) and 66K proteins] are indicated by arrows. Lanes 3 and 3′ correspond to C-terminal labeling conditions, under which the 69K is not labeled (Kadaré *et al.,* 1992). Translation products made from TYMV RNA were immunoprecipitated with the anti-66K antiserum and protein A–Sepharose and were analyzed by SDS–PAGE on another 7% polyacrylamide gel (lane 5).

the nomenclature of the C-terminal cleavage product used in earlier studies (Kadaré *et al.,* 1995; Bransom *et al.,* 1996).

## Accumulation of 66K protein and CP in TYMV-infected plants

The accumulation of the TYMV 66K protein in virus-infected *Arabidopsis* plants was studied in a time course experiment. A batch of plants was inoculated with TYMV and samples from inoculated plants were taken at various times postinoculation (p.i.). Total protein extracts were prepared and analyzed by Western blotting using anti-66K and anti-CP antisera (Figs. 3A and 3B). Accumulation of both proteins became detectable in *Arabidopsis* plants at 6 days p.i. (i.e., at the onset of leaf symptom development) and both proteins were detected for the remainder of the experiment. Since the samples consisted of whole plant material, it should be noted that synthesis of the viral proteins in newly infected apical leaves that emerge in the course of the experiment could compensate for the disappearance of viral proteins from tissue infected at earlier times.

To investigate the possibility that the viral proteins were expressed transiently upon infection, TYMV was inoculated on the lower leaves of Chinese cabbage plants. Two months p.i., each leaf from the infected plants was harvested separately and total proteins extracts were revealed by Western blotting using the anti-66K antibodies. As shown in Fig. 3C, the 66K protein was most abundant in the young, partially expanded systemically infected leaves, and its amount was found to decline as the leaf ages. Since the infections that we have followed were obviously nonsynchronous and cannot be

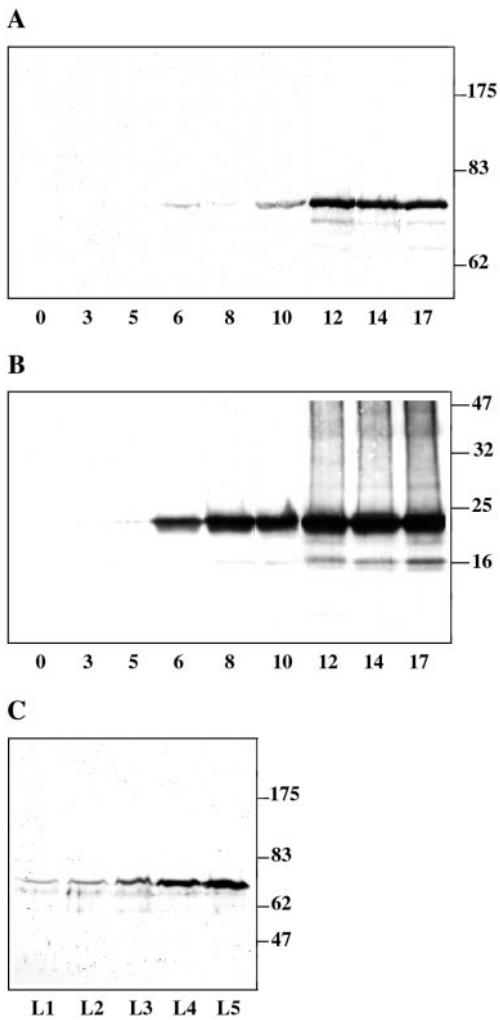


FIG. 3. Accumulation of the TYMV 66K protein and CP in infected plants. TYMV-infected *Arabidopsis* plants (A and B) were collected at 1–17 days p.i. (lanes 1–17) and TYMV-infected Chinese cabbage leaves (C) were collected at 2 month p.i., with each leaf being collected separately (lanes L1 to L5). Lane L1 corresponds to the older leaf and lane L5 to a small emerging one, with all leaves being symptomatic. Total proteins were extracted and equivalent amounts of proteins were analyzed by SDS–PAGE on 7 (A and C) or 15% (B) polyacrylamide gels. The gels were electroblotted onto a nitrocellulose filter and proteins were revealed by Western blotting using the anti-66K (A and C) or the anti-CP (B) antisera. Lane 0 corresponds to protein extracts from a noninfected *Arabidopsis* plant. The position of prestained molecular weight markers (Biolabs) is indicated.

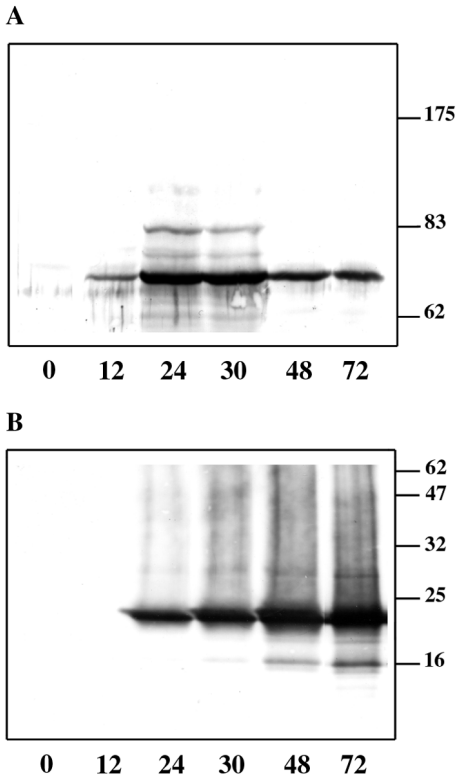


FIG. 4. Immunodetection of the TYMV 66K protein and CP in infected protoplasts. Samples of TYMV-infected *Arabidopsis* protoplasts were collected at 0, 12, 24, 30, 48, and 72 h p.i. (lanes 0, 12, 24, 30, 48, and 72) and equivalent amount of proteins were analyzed by SDS–PAGE on 7 (A) or 15% (B) polyacrylamide gels. The gels were electroblotted onto a nitrocellulose filter and proteins were revealed by Western blotting using the anti-66K (A) or the anti-CP (B) antisera. The position of prestained molecular weight markers (Biolabs) is indicated.

interpreted in terms of a single infection cycle, the kinetics of accumulation of the viral proteins was further studied in TYMV-infected protoplasts.

## Immunodetection of 66K protein and CP in TYMV-infected protoplasts

The accumulation of the 66K protein was analyzed after PEG-mediated transfection of *A. thaliana* protoplasts with TYMV viral RNA as described previously (Schirawski *et al.,* 2000). Samples were collected at various times p.i. and equivalent amounts of proteins were subjected to Western blot experiments using the anti-66K and anti-CP antibodies (Fig. 4). Kinetics experiments revealed that the 66K protein was first detected at 12 h p.i., reached maximal levels 24–30 h p.i., and then declined (Fig. 4A). A number of bands of higher molecular mass as well as putative degradation products were also detected using the anti-66K antibody. These forms were most prominent in midstages of infection and displayed the same transient expression pattern as the 66K protein. In contrast, the CP was first detected at 24 h p.i. and remained abundant throughout the experiment (Fig. 4B).

## Subcellular fractionation experiments

To investigate the subcellular localization of the 66K protein, TYMV-infected protoplasts were lysed to yield a total protein fraction, which was then subjected to fractionation by differential centrifugation, giving rise to P1, P30, and S30 subcellular fractions (Niesbach-Klösgen *et al.,* 1990; Hughes *et al.,* 1995). Samples corresponding to equivalent amounts of fresh tissue were subjected to SDS–PAGE, and after electrotransfer, immunoblots were probed for 66K protein and CP as before. As shown in Fig. 5A, the bulk of 66K protein was found in fraction P1 (containing nuclei, chloroplasts, and associated membranes) and P30 (membranes from the endoplasmic reticulum and dissociated organelles). The 66K protein was not detected in the cytoplasmic S30 fraction, which,

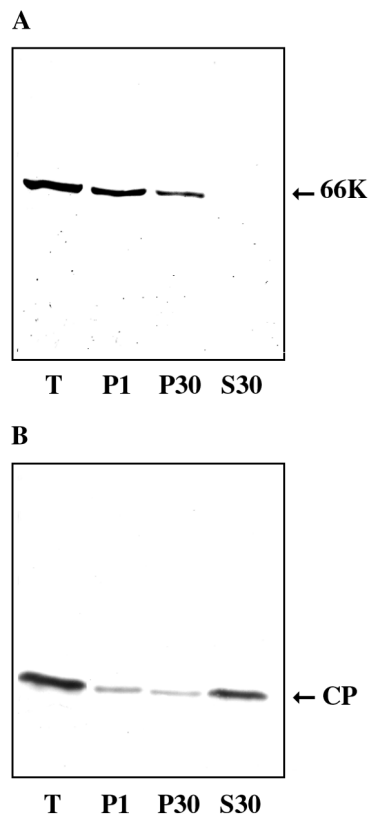


FIG. 5. Immunodetection of TYMV 66K protein and CP in different subcellular fractions of infected protoplasts. TYMV-infected protoplasts were harvested 22 h postinoculation and lysed to yield a total protein fraction (T) that was then subjected to fractionation by differential centrifugation, giving rise to a 1000 *g* pellet (P1) and to 30,000 *g* pellet and supernatant fractions (P30 and S30, respectively). Equal percentages of each fraction were analyzed by SDS–PAGE on 7 (A) or 15% (B) polyacrylamide gels. The gels were electroblotted onto a nitrocellulose filter and proteins were revealed by Western blotting using the anti-66K (A) or the anti-CP (B) antisera. The subcellular fractions should be enriched in the following structures: P1: nuclei, chloroplasts and starch granules; P30: rough endoplasmic reticulum, Golgi bodies, peroxisomes, chloroplast debris and mitochondria; S30: polysomes, large proteinaceous complexes, soluble proteins, and the cytosol.

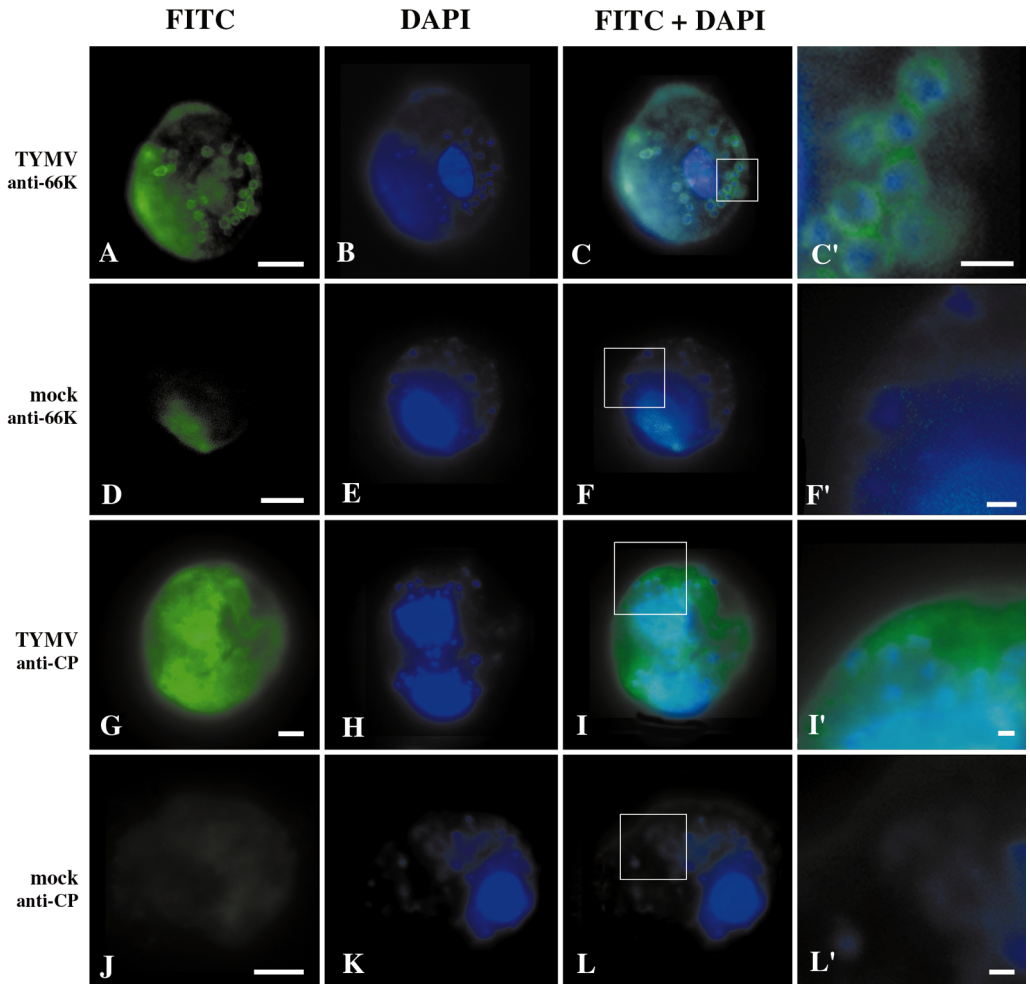


FIG. 6. Localization of TYMV 66K protein and CP in protoplasts using immunofluorescence labeling. Epifluorescence micrographs of TYMV-infected (A–C′, G–I′) or mock-infected (D–F′, J–L′) *Arabidopsis* protoplasts. The protoplasts were collected 24 h p.i. and processed for indirect immunofluorescence labeling using anti-66K (A–F) or anti-CP (G–L) antisera followed by secondary antibodies coupled to FITC. The nuclear and chloroplastic DNA was stained by DAPI. For each cell, the fluorescing protein (green) and DNA (blue) images were gathered simultaneously using standard FITC and DAPI filter settings and the images were digitally superimposed. Scale bars are 10 $\mu$m. The images C′, F′, I′, and L′ represent an enlargement of the boxed areas in the images C, F, I, and L, respectively (scale bars are 2 $\mu$m).

in contrast, was found to contain most of the CP (Fig. 5B). This finding is consistent with the accumulation of viral particles within the cytoplasm of the infected cells (Hatta and Matthews, 1976). CP was also detected in smaller quantities in the P1 and P30 fractions, possibly due to the presence of empty protein shells in the nucleus or to the accumulation of virus aggregates within spaces between clumped chloroplasts as reported previously (Ushiyama and Matthews, 1970; Hatta and Matthews, 1976).

### Localization of 66K protein and CP in TYMV-infected protoplasts by immunofluorescence microscopy

To analyze the intracellular sites of accumulation of TYMV 66K protein, indirect immunofluorescence microscopy was carried out on mock- or TYMV-infected protoplasts. After fixation, the protoplasts were probed with the anti-66K or anti-CP antibodies and secondary antibodies coupled to FITC while DNA from the nucleus and the organelles was counterstained using DAPI. Figure 6 shows representative epifluorescence micrographs of such cells. TYMV-infected cells displayed a bright fluorescent staining of the 66K protein (green) in the shape of rings or groups of rings scattered throughout the cytoplasm (Fig. 6A). These rings appeared to surround the chloroplasts, as revealed by the FITC (green) + DAPI (blue) overlay (Figs. 6C–6C′). Some weaker fluorescence signal was also observed throughout the cytoplasm of TYMV-infected cells as confirmed by confocal microscopy (data not shown). Mock-infected cells processed and imaged in parallel showed equivalent nuclear and chloroplastic DNA staining (Figs. 6D–6F′), but negligible fluorescence due to the anti-66K antiserum was de-

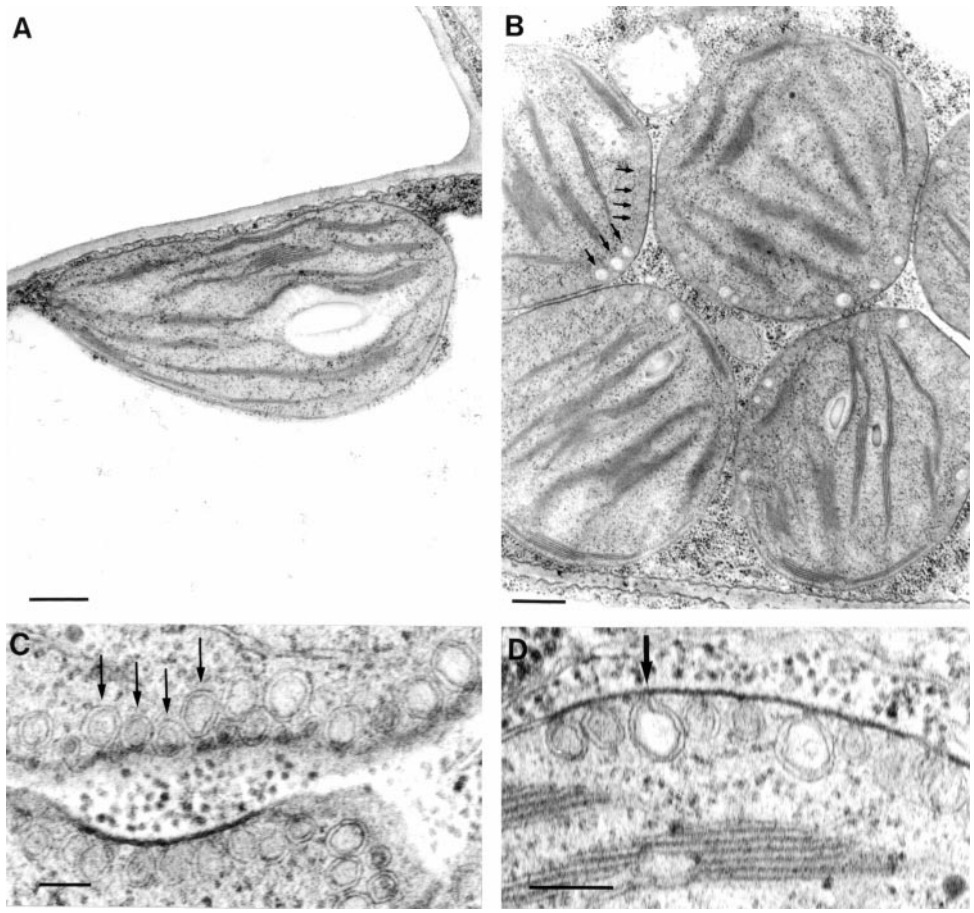


FIG. 7. Cytopathology of TYMV-infected cells. Ultrathin sections of chloroplasts from healthy (A) and TYMV-infected Chinese cabbage leaves (B–D). Thin arrows indicate vesicles at the chloroplast periphery and the thick arrow in D indicates a vesicle in which an open channel is apparently connecting the interior of the vesicle to the cytoplasm. The bar corresponds to 400 nm in A and B and to 100 nm in C and D.

tected. The anti-CP antiserum revealed that the capsid protein was localized throughout the cytoplasm of infected cells (Figs. 6G–6I′) but was absent from mock-infected cells (Figs. 6J–6L′). Occasionally, the CP was also observed to localize to punctate spots around the chloroplasts (data not shown).

### Localization of 66K protein in TYMV-infected plants by electron microscopy

To further examine the subcellular localization of the TYMV 66K protein, we performed electron microscopy examination of ultrathin sections prepared from apical leaf tissue of TYMV-infected Chinese cabbage (Fig. 7). The cytological abnormalities induced by TYMV infection appeared to be confined to the chloroplasts, confirming previous reports (Laflèche and Bové, 1969; Ushiyama and Matthews, 1970; Hatta *et al.,* 1973; Hatta and Matthews, 1974). In healthy control cells (Fig. 7A), the chloroplasts are oblong-shaped, whereas in infected cells (Fig. 7B) they appear swollen, rounded, and clumped together in groups forming "polyplasts" (Laflèche and Bové, 1969). Adjacent chloroplasts delimit cytoplasmic pockets that are often filled with TYMV particles. Most conspicuous is the presence of characteristic virus-induced small vesicles at the chloroplast peripheries (Figs. 7B–7D), which are particularly abundant beneath those areas of the chloroplast surface that are adjacent to other chloroplasts in a clump. These double membrane vesicles are morphologically similar to those described previously in detail (Laflèche and Bové, 1969; Ushiyama and Matthews, 1970; Hatta *et al.,* 1973) and they have been proposed to result from invaginations of the chloroplast envelope into the organelle (Laflèche and Bové, 1969; Hatta *et al.,* 1973).

The intracellular sites of accumulation of the TYMV 66K protein were localized by performing immunogold-labeling experiments. After ultrathin sectioning, healthy and TYMV-infected tissues were probed with anti-66K antibody and then with protein A coupled to 10-nm colloidal gold beads (Fig. 8). A study of the electron micrographs of leaf tissue sections that had been gold-labeled with anti-66K serum and the counting of the number of

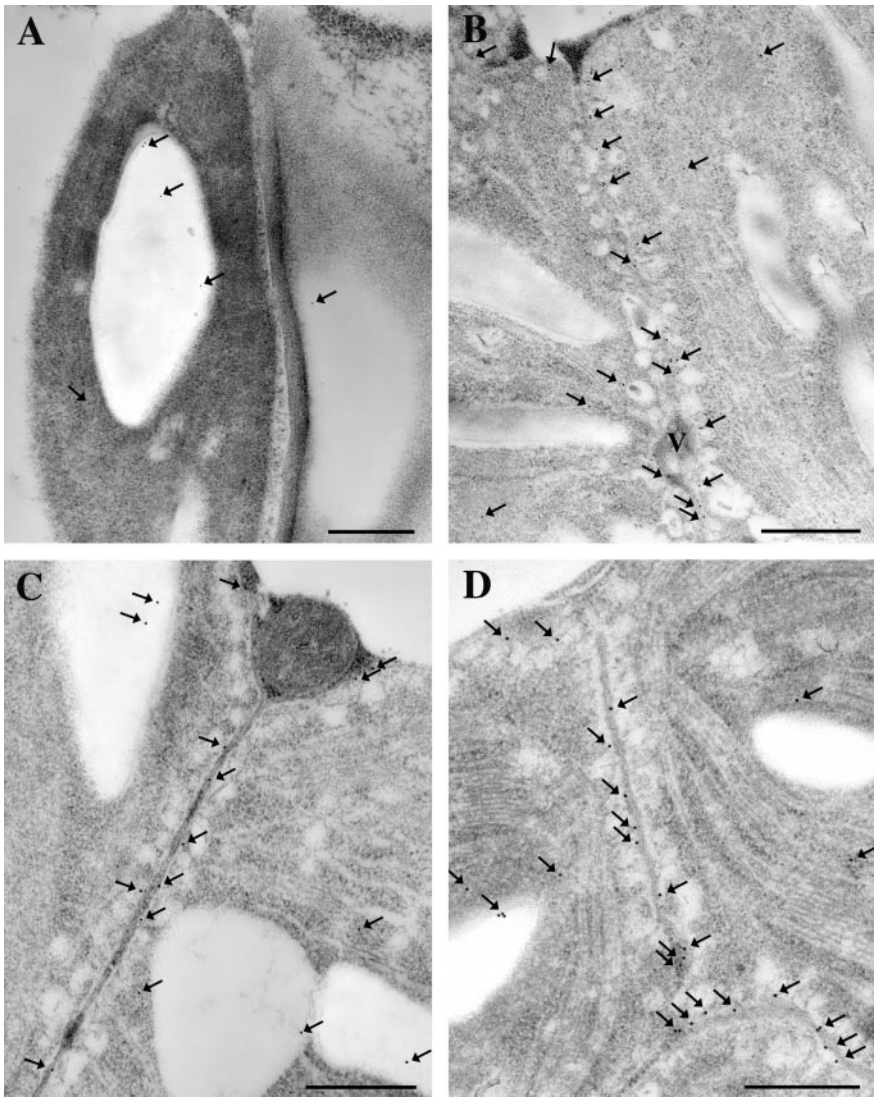


FIG. 8. Immunolocalization of the 66K protein in TYMV-infected cells. Typical images of immunogold labeling using anti-66K antiserum in ultrathin sections of chloroplasts from healthy (A) and TYMV-infected Chinese cabbage leaves (B–D). All the gold beads (10 nm in size) are indicated by arrows. The bar corresponds to 500 nm in A and B and to 400 nm in C and D. V indicates TYMV particles. Fields spanning adjacent clumped chloroplast envelopes were selected for examination at higher magnification (E–M). The bar corresponds to 100 nm.

gold granules present on sections of healthy or TYMV-infected leaves showed that the distribution of the beads on the surface of the cell sections was not random, since the largest amount of labeling was observed at the periphery of chloroplasts of the infected cells (Table 1). Thus in the fields from the inoculated leaves, on a total of 3511 beads enumerated, 1363 (38.8%) were associated with the chloroplast envelope, even though the areas occupied by these latter structures represented only 5.9% of the total surface examined. The remainder of the beads were distributed in an apparently random fashion over the other subcellular components, as in healthy control cells. Gold label was scarcely observed in the sections of TYMV-infected plants incubated with preimmune serum or buffer prior to the secondary antibody treatment (data not shown), demonstrating the specificity of the labeling.

Representative images of gold-decorated chloroplast envelopes observed in TYMV-infected leaves are shown in Figs. 8B–8D. Cells from healthy plants (Fig. 8A) did not display colloidal gold labeling at the chloroplast periphery. Crystallized masses of TYMV particles were visible in the cytoplasm or within cytoplasmic pockets between clumped chloroplasts in some of the sections from the infected leaves (see Fig. 8B, V) but no significant immunogold labeling of the viral particles by the anti-66K-specific antibody was observed. Fields spanning adjacent clumped chloroplast envelopes were selected for observation at higher magnification and are shown in Figs. 8E–8M. In the great majority of images, the gold

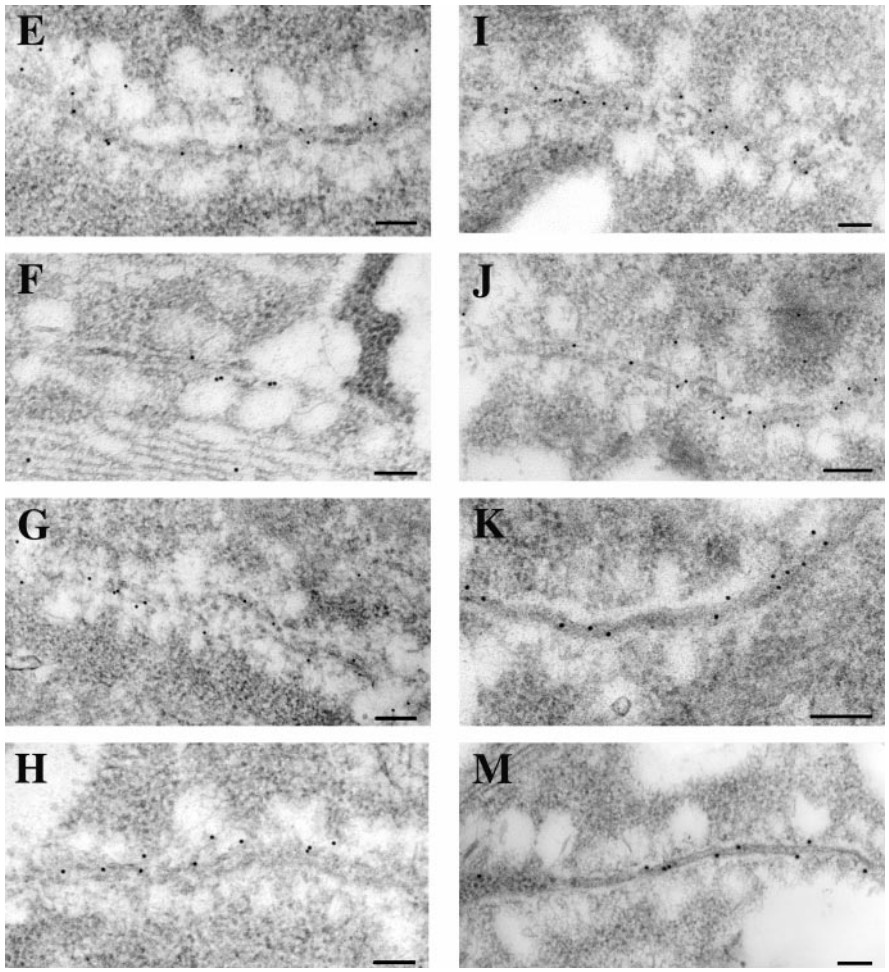


FIG. 8—*Continued*

beads appeared not to lie inside the vesicles but seemed rather to be apposed to the part connecting them to the chloroplast envelope, i.e., in proximity to the vesicle necks.

## DISCUSSION

### Proteolytic processing of the TYMV 206K protein *in vivo*

All RNA viruses known to date encode an RNA-dependent RNA polymerase that is required for replication of the viral genome (reviewed in Buck, 1996). Our results indicate that the TYMV RdRp domain is present *in planta* within a single major ~66-kDa protein product (Fig. 1). This confirms that the 206K nonstructural protein undergoes proteolytic processing *in vivo* to generate discrete polypeptides carrying functionally distinct domains presumably active in viral replication. Based on its apparent molecular mass, gel mobility, and antibody recognition (Fig. 2), we assume that the 66-kDa product identified in infected plants is similar to the 66K protein previously described as the C-terminal cleavage product of the 206K protein translated *in vitro* (Morch *et al.,* 1989; Bransom *et al.,* 1991). Considering the importance of the papain-like proteinase for the *in vitro* processing of the 206K protein (Bransom and Dreher, 1994; Rozanov *et al.,* 1995) and its indispensability for TYMV replication in protoplasts (Bransom and Dreher, 1994), this domain is likely to be involved in the cleavage process giving rise to the 66K protein *in planta.* Alternatively, the cleavage may be mediated *in trans* by a host enzyme. Proteolysis of a large nonstructural polyprotein to yield a "methyltransferase-helicase" block as an N-terminal product and a separate RNA polymerase protein as a C-terminal product is presumably important in the life cycle of a number of viruses belonging to the "alpha-like" supergroup since it has been reported to occur *in vivo* in members of the rubi-, carla-, and benyviruses (Marr *et al.,* 1994; Lawrence *et al.,* 1995; Hehn *et al.,* 1997). Similar proteolytic processing of translation products *in vitro* has also been reported for additional members of the tymo-

TABLE 1

66K-Specific Immunogold Labeling of Different Subcellular Structures in Healthy and TYMV-Infected Plants

| | Healthy leaves | | | TYMV-infected leaves | | |
|---|---|---|---|---|---|---|
| Cell wall and plasma membrane | 117[a] | 201[b] | 0.58[c] | 105[a] | 109[b] | 0.96[c] |
| Vacuole | 1118 | 1645 | 0.68 | 862 | 1265 | 0.68 |
| Chloroplast envelope | 49 | 79 | 0.62 | 1363 | 125 | 10.90 |
| Chloroplast stroma and starch grains | 622 | 633 | 0.98 | 1050 | 532 | 1.97 |
| Nucleus, cytoplasm, and other organelles | 295 | 337 | 0.87 | 131 | 81 | 1.61 |
| Total | 2201 | 2895 | | 3511 | 2112 | |

[a] Total number of gold particles decorating different subcellular structures.

[b] Total surface ($\mu m^2$) occupied by the corresponding structure (in infected cells, the surface of the vesicles has been included in the chloroplast envelope surface).

[c] Density of gold particles (number per $\mu m^2$) within the corresponding structure.

and carlaviruses (Kadaré *et al.,* 1992; Foster and Mills, 1992).

Probing of protein blots of infected protoplasts with anti-66K antibodies (Fig. 4) resulted in the detection of multiple bands of higher molecular mass that were most prominent in midstages of infection and displayed a transient expression pattern. We do not know at this time whether this is due to cross-reactivity of the antibodies with host proteins induced upon infection, to alternative proteolytic cleavage(s), or to posttranslational modification(s) of the 66K protein. In any case, the cleavage event that generates the 66K protein from the 206K protein must occur rapidly *in vivo* as no 206K species could be immunodetected by Western blot even at earlier times p.i. (data not shown).

In the protoplast samples collected at later times postinoculation (Fig. 4) as well as in infected plants (Figs. 1 to 3), the absence of immunoreactive higher molecular mass species indicates that the 66K protein is the only viral protein containing the RdRp domain that accumulates in a stable form. We cannot exclude, however, the possibility that additional cleavage sites may exist within the 206K protein and give rise to transiently expressed species that went undetected in the infected plants. In that respect, it should be noted that the proteinase domain of alphaviruses is responsible for producing the mature viral proteins using multiple sequential *cis* and *trans* cleavages (reviewed in Strauss and Strauss, 1994) that appeared to play a pivotal role in the temporal regulation of minus- and plus-strand RNA synthesis of Sindbis virus (Lemm *et al.,* 1994). This raises the question of whether a similar processing scheme may occur in TYMV as well. In support of this, it is worth noting that previously purified TYMV replicase fractions were shown to contain a 115-kDa protein of viral origin that is likely to arise from the processing of the 206K protein (Mouchès *et al.,* 1984; Candresse *et al.,* 1986). The origin of this 115-kDa polypeptide is still unclear although it has been proposed to contain both the NTPase/helicase and the RdRp protein domains (Deiman *et al.,* 1997). However, using the antibody we raised against the TYMV RdRp domain, we have been unable to detect a protein this size in infected plants or protoplasts. It remains to be determined whether this apparent discrepancy reflects a difference in protein composition between the purified replicase fractions and the total protein samples or whether it is due to differences in antisera specificity. We are currently raising antibodies against areas in the remaining 140K N-terminal region of the polyprotein and future studies will focus on the analysis of the products present in infected plant cells to determine the processing strategy and the function of the mature protein(s). This may help clarify the origin of the 115-kDa polypeptide found in purified TYMV replicase preparations.

### Transient accumulation of the 66K protein

The time course of appearance of the 66K protein in plants (Fig. 3) revealed that the protein is expressed early in infection and that the level of detectable protein declines steadily as the leaves mature. This observation is consistent with the observed peak of RdRp activity purified from Chinese cabbage leaves (Deiman *et al.,* 1997) and the expected role of the 66K protein in viral RNA replication. Because of the obvious difficulties associated with analysis of timing in infected leaves, the accumulation kinetics of the 66K protein was followed during synchronous infection of *Arabidopsis* protoplasts (Fig. 4). These results revealed that the 66K protein accumulates transiently, reaching the maximal level between 24 and 30 h.p.i. These observations are in good agreement with earlier studies regarding the kinetics of accumulation of the replication-related proteins of other plant viruses from the alpha-like supergroup (Joshi *et al.,* 1983; Watanabe *et al.,* 1984; Berna *et al.,* 1986; van Pelt-Heerschap *et al.,* 1987; Hehn *et al.,* 1997).

Several explanations can be proposed to account for the apparent decay of the TYMV 66K protein. Because

protoplast samples were adjusted for equivalent protein concentration before Western blot analysis, it is very unlikely that the fall-off of the 66K protein at 32–48 h p.i. simply reflects protoplast mortality. Since the amount of protein observed is the balance between its synthesis and its decay, the observed disappearance of the 66K protein may reflect the cessation of its synthesis. Changes in the proteolytic processing of the 206K protein are also conceivable, although no other protein products encompassing the RdRp domain were recognizable to our antibodies. Alternatively, the 66K protein could be cleaved by proteases or degraded. Indeed a number of faint bands, which could correspond to degradation products, are usually visible on our immunoblots. In that respect, it should be emphasized that the TYMV 66K protein has recently been shown to be phosphorylated and ubiquitinylated when expressed in insect cells (Héricourt *et al.,* 2000). Ubiquitinylation is a common means used by eukaryotic cells to signal unstable proteins for their subsequent degradation by the 26S proteasome, a multiprotease complex (reviewed in Ciechanover, 1998). Experiments in progress should allow us to determine whether the metabolic stability of the TYMV 66K protein may be controlled through the ubiquitin-dependent proteasome pathway in plants.

### Localization of the TYMV 66K protein

The observed subcellular distribution of the TYMV 66K protein in the membrane fraction of infected cells (Fig. 5) agrees well with that of other RNA virus replication-associated enzymes, which are most often found associated with membranous structures (reviewed in David *et al.,* 1992; Scholthof *et al.,* 1995; Restrepo-Hartwig and Ahlquist, 1996; Schaad *et al.,* 1997; Mas and Beachy, 1999; Erokhina *et al.,* 2000). The assembly of a multiprotein replication complex on intracellular membranes thus seems to be a general aspect of positive-strand RNA virus replication, in both plants and animals. However, there also appear to be diversities in the type of cellular membrane where the viral replication complexes are localized (reviewed in Buck, 1996). The immunofluorescence microscopy experiments presented in this study (Fig. 6) demonstrate that the 66K protein carrying the RdRp domain localizes to the chloroplast periphery. This result is fully consistent with previous *in vivo* RNA labeling observations (Laflèche and Bové, 1969; Laflèche *et al.,* 1972; Garnier *et al.,* 1980) and immunocytochemical experiments using anti-replicase antibodies (Garnier *et al.,* 1986), suggesting that replication of TYMV RNA is associated with the chloroplast envelope.

The cytopathology induced by TYMV infection as visualized by electron microscopy (Fig. 7) is in remarkable agreement with the early work on TYMV (reviewed in Matthews, 1973). The infected cells exhibited formation of vesicles that are characteristic of TYMV infection (Laflèche and Bové, 1969; Ushiyama and Matthews, 1970; Hatta *et al.,* 1973; Hatta and Matthews, 1974) and that have been proposed to constitute the site of viral replication (Ushiyama and Matthews, 1970; Matthews, 1973). Based on the examination of leaf tissue by immunocytochemistry (Fig. 8), we present evidence that the 66K protein accumulates preferentially at the edge of these membrane vesicles. Our present finding therefore bears out the notion that these vesicular structures are very likely to represent the actual TYMV replication sites.

The association of viral RNA synthesis with cellular membranes in eukaryotic cells is an intriguing phenomenon, from both a functional and a mechanistic point of view. Despite their central role in viral pathology, little is known about the molecular mechanisms allowing the formation of viral replication complexes and their anchoring in cellular membranes. The vesicles at the chloroplast periphery of TYMV-infected cells were first described in 1966 (Chalcroft and Matthews, 1966), but information concerning the origin and biogenesis of these vesicles is still missing. Defining those mechanisms will give new insights about the specific virus–host interactions that ultimately determine a successful viral infection.

## MATERIALS AND METHODS

### Hosts and virus

Chinese cabbage (*Brassica pekinensis* cv. Granaat) and *A. thaliana* (cv. C24) were grown from seeds at 20–25°C with a 16-h daylength. Plants were mechanically inoculated on four of the lower well-expanded leaves using an inoculum consisting of infected leaf tissue freshly homogenized in 20 mM sodium phosphate, pH 7.5 (4 ml/g). Virus and viral RNA were prepared by standard methods (Matthews, 1960).

### Tissue extraction

Healthy or TYMV-infected leaf samples were collected at various times postinoculation and total proteins were isolated by grinding the plant material with a mortar and pestle with 5 ml of extraction buffer (150 mM Tris–HCl, pH 6.8, 8% SDS, 2 M $\beta$-mercaptoethanol, 30% glycerol) per gram of fresh weight. Whole *Arabidopsis* plants and individual leaves of Chinese cabbage plants were collected. Samples were clarified by centrifugation for 5 min at 13,000 *g,* boiled for 10 min, and subjected to SDS–PAGE.

### Antisera

The polyclonal antiserum against the TYMV 66K protein was raised by injecting rabbits with purified recombinant histidine-tagged 66K protein (His-66K) expressed

in the baculovirus insect cell system (Héricourt *et al.,* 2000). The protein was solubilized in 8 M urea and purified on Ni-NTA resin as described previously (Héricourt *et al.,* 2000). The generation of rabbit antiserum was performed by Eurogentec according to the standard immunization protocol using 100 $\mu$g of purified His-66K per injection.

To eliminate any nonspecific reactions, in particular against compounds present in the extraction buffer, the anti-66K antiserum was preadsorbed by overnight incubation at 4°C with a nitrocellulose membrane on which extraction buffer had been spotted.

The antiserum against the TYMV capsid was described previously (Garnier *et al.,* 1986) and was kindly provided to us by T. Candresse, INRA Bordeaux, Bordeaux, France. To remove nonspecific reactions in Western blotting experiments, the anti-CP antiserum was preadsorbed by overnight incubation at 4°C with a nitrocellulose membrane on which total protein extracts from uninfected *A. thaliana* cells had been electrotransfered.

### Preparation and inoculation of protoplasts

Protoplasts were prepared from a cell suspension culture of *A. thaliana* and transfected as described previously (Schirawski *et al.,* 2000). Viral RNA (2 $\mu$g) was used to inoculate approximately $10^6$ protoplasts. Following inoculation, the protoplasts were incubated in the dark at 24°C for the periods indicated. The protoplasts were collected by centrifugation at 80 *g* for 10 min at room temperature (RT) and rinsed in PBS containing a mixture of protease inhibitors (Complete protease inhibitor cocktail, Roche) prior to further analyses.

### Subcellular fractionation

TYMV-infected protoplasts were harvested for subcellular fractionation at 18–24 h posttransfection. Following the washing step, $\sim 5 \times 10^6$ protoplasts were resuspended in 1 ml of buffer E (100 mM Tris–HCl, pH 7.5, 10 mM KCl, 5 mM $MgCl_2$, 400 mM saccharose, 10% glycerol, 10 mM $\beta$-mercaptoethanol) containing a mixture of protease inhibitors (Complete protease inhibitor cocktail, Roche) and were lysed by 20 passages through a 23-gauge syringe needle. Subcellular fractionation was performed by differential centrifugation according to Niesbach-Klosgen *et al.* (1990), giving rise to a 1000 *g* pellet (P1) and to 30,000 *g* pellet and supernatant fractions (P30 and S30, respectively). Proteins in the P1 and P30 pellets were solubilized in extraction buffer and samples of each subcellular fraction corresponding to the same amount of fresh tissue were subjected to SDS–PAGE.

### Immunofluorescence labeling

TYMV- or mock-infected protoplasts ($\sim 10^6$ cells) were harvested for immunofluorescence staining at 18–24 h posttransfection. The protoplasts were allowed to settle on poly-L-lysine-coated coverslips for 20 min at RT and were then fixed by immersion of the slides in cold 95% ethanol for 20 min. After incubation for 45 min at RT in blocking solution (5% BSA in PBS), the cells were incubated for 1 h at 37°C with the primary antibody diluted 1/500 in PBS, 1% BSA. After three washes for 5 min in PBS, 0.2% Tween 20, the cells were incubated in the dark for 30 min at 37°C with a FITC-conjugated goat anti-rabbit IgG (Jackson ImmunoResearch Laboratories) diluted 1/150 in PBS, 1% BSA. After incubation with $10^{-4}$ M DAPI for DNA staining, the cells were washed once in PBS, 0.2% Tween 20 and the coverslips were mounted on microscope slides using citifluor. Fluorescence microscopy was carried out with an epifluorescence microscope (Leica HBO 100) or with a confocal microscope (Leica TCS 4D) equipped with a 63× objective. Standard filters for FITC and DAPI were used to detect fluorochromes. Images were captured with a CCD camera (Princeton Instruments Inc.) driven by the software Metaview (Metaview Imaging System). They were processed by Photoshop (Adobe Systems) for color level and contrast adjustment.

### Protein analysis

The protein concentration was determined by disrupting samples corresponding to $\sim 10^5$ protoplasts in 40 mM Tris–HCl, pH 8, 100 mM NaPi, 6 M guanidinium–HCl for 1 h at RT, followed by a 50× dilution in Coomassie Protein Assay Reagent (Pierce) and reading the absorbance at 595 nm using BSA as a reference.

Proteins for Western blot analysis were prepared by mixing pelleted protoplasts corresponding to identical amounts of total proteins with 1/3 vol of extraction buffer followed by boiling for 3 min immediately prior to electrophoresis. For detection of the 66K protein, samples consisting of 10 $\mu$g of total proteins or 2 mg of fresh plant material were separated by 7% SDS–PAGE (Laemmli, 1970), while for detection of the CP, 2 $\mu$g of total proteins or 10 $\mu$g of fresh plant material was separated by 15% SDS–PAGE. After electrotransfer to nitrocellulose membranes using a semidry apparatus, the protein blots were allowed to react overnight at 4°C with preadsorbed anti-66K or anti-CP antibodies (dilution 1/1000) in PBS, 0.05% Tween 20, and 5% nonfat powdered milk. After washes in PBS, 0.05% Tween 20, the membranes were incubated for 2 h at room temperature with PBS, 0.05% Tween 20, and 5% nonfat powdered milk containing a 1/30,000 dilution of goat anti-rabbit IgG coupled to alkaline phosphatase (Sigma). After additional washing steps in PBS, 0.05% Tween 20, the membranes were incubated with NBT-BCIP as substrates.

### *In vitro* translation and immunoprecipitation

The cDNA sequence encoding the 66K protein product (nt 3872–5629 according to Morch *et al.,* 1988) was amplified by PCR using the cDNA clone p17AE (Héricourt *et al.,* 2000) as a template, with the positive-sense primer, 5′ TAATACGACTCACTATAGGGAGACCACATGGGCACCCCCAGCGCATCCCCCACC 3′, which provided a T7 promoter (underlined) at the 5′ terminus of the gene and the negative-sense primer, 5′ CGGGATCCGGTACCCTATTGGACGTAGTGAAGCAATTC 3′. The resulting DNA fragment (T7-66K) was *in vitro* transcribed and translated in the TNT T7 Quick Coupled Transcription/Translation system (Promega) according to the supplier's instructions. The standard translation conditions of TYMV RNA (250 ng of RNA in a 10-$\mu$l total volume) using a nuclease-treated rabbit reticulocyte lysate were described previously (Morch *et al.,* 1989) except that 530 MBq of a mixture of L-[$^{35}$S]methionine and L-[$^{35}$S]cysteine (Pro-Mix, Amersham) was used to label the proteins. Incubations were performed at 30°C for 60 min. C-terminal labeling experiments were performed as described in Kadaré *et al.* (1992). Briefly, the translation reactions were initiated in the absence of radiolabeled amino acid and after 10 min, edeine (20 $\mu$M, final concentration) was added to block further initiation of polypeptide chains. Thirty minutes after the onset of incubation, L-[$^{35}$S]methionine and L-[$^{35}$S]cysteine were added to label the C-terminal regions of the proteins, and incubation was continued for a total of 90 min. The $^{35}$S-labeled products were separated by 7% SDS–PAGE, transferred to nitrocellulose, visualized by autoradiography, and then processed for immunoblot analysis using the anti-66K antiserum.

For immunoprecipitation, the translation mixture (10 $\mu$l) was mixed with an equal volume of extraction buffer and boiled for 3 min. The sample was then diluted with 180 $\mu$l of IP buffer (50 mM Tris–HCl, pH 7.5, 150 mM NaCl, 5 mM EDTA, 0.1% SDS, 1% Triton X-100, and 0.1% BSA) and 0.5 $\mu$l of the anti-66K antiserum. After overnight incubation at 4°C, the antigen–antibody complexes were precipitated with protein A–Sepharose (Amersham) that had been preadsorbed with unprogrammed rabbit reticulocyte lysate. After several washes in Super-wash buffer (50 mM Tris–HCl, pH 7.5, 100 mM NaCl, 2 mM EDTA, 0.5% SDS, 2% Triton X-100), the immunoprecipitates were removed from the protein A–Sepharose by boiling in extraction buffer, separated by 7% SDS–PAGE, and visualized by autoradiography.

### Processing of leaf tissues

For ultrastructure observation, systemically infected Chinese cabbage leaf tissue and a noninoculated control were harvested and tissues were cut into 2 × 0.5 mm strips under fixative (3% glutaraldehyde and 1% tannic acid buffered to pH 7.4 with 0.1 M sodium cacodylate buffer) and left for 3 h at 15°C in the fixative. They were then postfixed in 2% osmium tetroxide, stained with 0.5% uranyl acetate for 2 h at 4°C, dehydrated with a graded series of ethanol, and embedded in Spurr resin. Polymerization was carried out at 60°C for 24 h. Ultrathin serial sections were cut with a diamond knife on an ultramicrotome and were mounted on copper grids. After staining with 2% uranyl acetate for 15 min and 2% lead citrate for 5 min, electron microscopy was carried out in a Philips EM410 electron microscope.

For immunogold experiments, the samples were fixed with a mixture of 4% paraformaldehyde and 0.5% glutaraldehyde in 0.1 M sodium cacodylate buffer at pH 7.4, dehydrated by increasing ethanol series, and embedded in LR white resin at low temperature in Leica EM AFS. Polymerization was carried out for 3 days at −20°C under long-wavelength UV light. Ultrathin serial sections were cut with a diamond knife on an ultramicrotome and were mounted on formvar-coated nickel grids for immunolabeling.

### Immunogold cytochemistry

Indirect immunogold labeling was carried out by floating the grids carrying serial tissue sections for 30 min at RT in PBS, 50 mM $NH_4Cl$. After incubation for 30 min at RT in blocking solution (5% BSA and 1% fish gelatin in PBS), the grids were incubated for 2 h at 4°C with the primary antibody diluted 1/300 in PBS, 1% BSA, 0.2% fish gelatin. The grids were washed three times for 5 min with PBS, 0.5% BSA, 0.1% fish gelatin and incubated for 45 min with protein A conjugated to 10-nm colloidal gold particles that had been diluted in PBS, 1% BSA, 0.2% fish gelatin. Preimmune serum was used at the same dilution as its corresponding antiserum (1/300). After extensive washing with PBS and ultrapure water, sections were stained with 2% uranyl acetate and 2% lead acetate, and electron microscopy was carried out in a Philips EM410 electron microscope. Counting of colloidal gold particles was done on 12 randomly chosen areas from healthy and TYMV-infected tissue.

## ACKNOWLEDGMENTS

We are grateful to Jan Schirawski and Anne-Lise Haenni for providing to us the *A. thaliana* suspension culture and for their help in the protoplast preparation and transfection system. We thank Thierry Candresse for the gift of anti-CP antibodies, Maria Savino, Marie-Aline Ludosky-Arnassalon, and Christiane Stussi-Garaud for useful advice, Gérard Géraud for his expertise in confocal microscopy, and Leonie van Dinten for comments on the manuscript. D.P. was the recipient of a Fellowship from the Ministère de l'Education Nationale, de la Recherche et de la Technologie (MENRT). This work was supported in part by grants from MENRT (Programme de Recherche Fondamentale en Microbiologie et Maladies Infectieuses et Parasitaires) and CNRS (Programme Jeunes Equipes) to I.J.

## REFERENCES


Bénicourt, C., and Haenni, A. L. (1978). Differential translation of turnip yellow mosaic virus mRNAs *in vitro*. *Biochem. Biophys. Res. Commun.* **84,** 831–839.

Berna, A., Briand, J. P., Stussi-Garaud, C., and Godefroy-Colburn, T. (1986). Kinetics of accumulation of the three non-structural proteins of alfalfa mosaic virus in tobacco plants. *J. Gen. Virol.* **67,** 1135–1147.

Bransom, K. L., and Dreher, T. W. (1994). Identification of the essential cysteine and histidine residues of the turnip yellow mosaic virus protease. *Virology* **198,** 148–154.

Bransom, K. L., Wallace, S. E., and Dreher, T. W. (1996). Identification of the cleavage site recognized by the turnip yellow mosaic virus protease. *Virology* **217,** 404–406.

Bransom, K. L., Weiland, J. J., and Dreher, T. W. (1991). Proteolytic maturation of the 206-kDa nonstructural protein encoded by turnip yellow mosaic virus RNA. *Virology* **184,** 351–358.

Buck, K. (1996). Comparison of the replication of positive-stranded RNA viruses of plants and animals. *Adv. Virus Res.* **47,** 159–251.

Candresse, T., Mouchès, C., and Bové, J. M. (1986). Characterization of the virus encoded subunit of turnip yellow mosaic virus RNA replicase. *Virology* **152,** 322–330.

Chalcroft, J., and Matthews, R. E. F. (1966). Cytological changes induced by turnip yellow mosaic virus in Chinese cabbage leaves. *Virology* **28,** 555–562.

Ciechanover, A. (1998). The ubiquitin–proteasome pathway: On protein death and cell life. *EMBO J.* **17,** 7151–7160.

David, C., Gargouri-Bouzid, R., and Haenni, A. L. (1992). RNA replication of plant viruses containing an RNA genome. *Prog. Nucleic Acid Res. Mol. Biol.* **42,** 157–227.

Deiman, B. A., Séron, K., Jaspars, E. M., and Pleij, C. W. A. (1997). Efficient transcription of the tRNA-like structure of turnip yellow mosaic virus by a template-dependent and specific viral RNA polymerase obtained by a new procedure. *J. Virol. Methods* **64,** 181–195.

Erokhina, T. N., Zinovkin, R. A., Vitushkina, M. V., Jelkmann, W., and Agranovsky, A. A. (2000). Detection of beet yellows closterovirus methyltransferase-like and helicase-like proteins *in vivo* using monoclonal antibodies. *J. Gen. Virol.* **81,** 597–603.

Foster, G. D., and Mills, P. R. (1992). Translation of potato virus S RNA *in vitro:* Evidence of protein processing. *Virus Genes* **6,** 47–52.

Garnier, M., Candresse, T., and Bové, J. M. (1986). Immunocytochemical localization of TYMV-coded structural and nonstructural proteins by the Protein A–gold technique. *Virology* **151,** 100–109.

Garnier, M., Mamoun, R., and Bové, J. M. (1980). TYMV RNA replication *in vivo:* Replicative intermediate is mainly single stranded. *Virology* **104,** 357–374.

Goldbach, R., and Wellink, J. (1988). Evolution of plus-strand RNA viruses. *Intervirology* **29,** 260–267.

Gorbalenya, A. E., Koonin, E. V., Donchenko, A. P., and Blinov, V. M. (1989). Two related superfamilies of putative helicases involved in replication, recombination, repair and expression of DNA and RNA genomes. *Nucleic Acids Res.* **17,** 4713–4730.

Hatta, T., Bullivant, S., and Matthews, R. E. F. (1973). Fine structure of vesicles induced in chloroplasts of Chinese cabbage leaves by infection with turnip yellow mosaic virus. *J. Gen. Virol.* **20,** 37–50.

Hatta, T., and Matthews, R. E. F. (1974). The sequence of early cytological changes in Chinese cabbage leaf cells following systemic infection with turnip yellow mosaic virus. *Virology* **59,** 383–396.

Hatta, T., and Matthews, R. E. (1976). Sites of coat protein accumulation in turnip yellow mosaic virus-infected cells. *Virology* **73,** 1–16.

Hehn, A., Fritsch, C., Richards, K. E., Guilley, H., and Jonard, G. (1997). Evidence for *in vitro* and *in vivo* autocatalytic processing of the primary translation product of beet necrotic yellow vein virus RNA 1 by a papain-like proteinase. *Arch. Virol.* **142,** 1051–1058.

Héricourt, F., Blanc, S., Redeker, V., and Jupin, I. (2000). Evidence for phosphorylation and ubiquitinylation of the turnip yellow mosaic virus RNA-dependent RNA polymerase domain expressed in a baculovirus-insect cell system. *Biochem. J.* **349,** 417–425.

Hughes, R. K., Perbal, M. C., Maule, A. J., and Hull, R. (1995). Evidence for proteolytic processing of tobacco mosaic virus movement protein in *Arabidopsis thaliana*. *Mol. Plant–Microbe Interact.* **5,** 658–665.

Joshi, S., Pleij, C. W. A., Haenni, A. L., Chapeville, F., and Bosch, L. (1983). Properties of the tobacco mosaic virus intermediate length RNA-2 and its translation. *Virology* **127,** 100–111.

Kadaré, G., Drugeon, G., Savithri, H. S., and Haenni, A. L. (1992). Comparison of the strategies of expression of five tymovirus RNAs by *in vitro* translation studies. *J. Gen. Virol.* **73,** 493–498.

Kadaré, G., Rozanov, M. N., and Haenni, A. L. (1995). Expression of the turnip yellow mosaic virus proteinase in *Escherichia coli* and determination of the cleavage site within the 206 kDa protein. *J. Gen. Virol.* **76,** 2853–2857.

Kamer, G., and Argos, P. (1984). Primary structural comparison of RNA-dependent polymerases from plant, animal and bacterial viruses. *Nucleic Acids Res.* **12,** 7269–7282.

Laemmli, U. K. (1970). Cleavage of structural proteins during the assembly of the head of bacteriophage T4. *Nature* **227,** 680–685.

Laflèche, D., and Bové, C. (1969). Development of double membrane vesicles in chloroplasts from turnip yellow mosaic virus infected cells. *Prog. Photosyn. Res.* **1,** 74–83.

Laflèche, D., Bové, C., Dupont, G., Mouchès, C., Astier, T., Garnier, M., and Bové, J. M. (1972). Site of viral RNA replication in the cells of higher plants: TYMV RNA synthesis on the chloroplast outer membrane system. In "Proceedings of the 8th FEBS meeting, Amsterdam, RNA viruses/ribosomes," Vol. 27, pp. 43–71. North-Holland Publishing, Amsterdam.

Lawrence, D., Rozanov, M. N., and Hillman, B. (1995). Autocatalytic processing of the 223-kDa protein of blueberry scorch carlavirus by a papain-like proteinase. *Virology* **207,** 127–135.

Lemm, J. A., Rumenapf, T., Strauss, E. G., Strauss, J. H., and Rice, C. M. (1994). Polypeptide requirements for assembly of functional Sindbis virus replication complexes: A model for the temporal regulation of minus- and plus-strand RNA synthesis. *EMBO J.* **13,** 2925–2934.

Marr, L. D., Wang, C. Y., and Frey, T. K. (1994). Expression of the rubella virus nonstructural protein ORF and demonstration of proteolytic processing. *Virology* **198,** 586–592.

Mas, P., and Beachy, R. N. (1999). Replication of tobacco mosaic virus on endoplasmic reticulum and role of the cytoskeleton and virus movement protein in intracellular distribution of viral RNA. *J. Cell Biol.* **147,** 945–958.

Matthews, R. E. F. (1960). Properties of nucleoprotein fractions isolated from turnip yellow mosaic virus preparations. *Virology* **12,** 521–539.

Matthews, R. E. F. (1973). Induction of disease by viruses, with special reference to turnip yellow mosaic virus. *Annu. Rev. Phytopath.* **11,** 147–170.

Morch, M. D., Boyer, J. C., and Haenni, A. L. (1988). Overlapping open reading frames revealed by complete nucleotide sequencing of turnip yellow mosaic virus genomic RNA. *Nucleic Acids Res.* **16,** 6157–6173.

Morch, M. D., Drugeon, G., Szafranski, P., and Haenni, A. L. (1989). Proteolytic origin of the 150-kilodalton protein encoded by turnip yellow mosaic virus genomic RNA. *J. Virol.* **63,** 5153–5158.

Mouchès, C., Candresse, T., and Bové, J. M. (1984). Turnip yellow mosaic virus RNA-replicase contains hosts and virus-encoded subunits. *Virology* **134,** 78–90.

Niesbach-Klösgen, U., Guilley, H., Jonard, G., and Richards, K. (1990). Immunodetection *in vivo* of beet necrotic yellow vein virus-encoded proteins. *Virology* **178,** 52–61.

Pleij, C. W. A., Neeleman, A., van Vloten-Doting, L., and Bosch, L. (1976). Translation of turnip yellow mosaic virus RNA *in vitro:* A closed and

an open coat protein cistron. *Proc. Natl. Acad. Sci. USA* **73,** 4437–4441.

Restrepo-Hartwig, M. A., and Ahlquist, P. (1996). Brome mosaic virus helicase- and polymerase-like proteins colocalize on the endoplasmic reticulum at sites of viral RNA synthesis. *J. Virol.* **70,** 8908–8916.

Rozanov, M. N., Drugeon, G., and Haenni, A.-L. (1995). Papain-like proteinase of turnip yellow mosaic virus: A prototype of a new viral proteinase group. *Arch. Virol.* **140,** 4545–4552.

Rozanov, M. N., Koonin, E. V., and Gorbalenya, A. E. (1992). Conservation of the putative methyltransferase domain: A hallmark of the 'Sindbis-like' supergroup of positive-strand RNA viruses. *J. Gen. Virol.* **73,** 2129–2134.

Schaad, M. C., Jensen, P. E., and Carrington, J. C. (1997). Formation of plant RNA virus replication complexes on membranes: Role of an endoplasmic reticulum-targeted viral protein. *EMBO J.* **16,** 4049–4059.

Schirawski, J., Planchais, S., and Haenni, A. L. (2000). An improved protocol for the preparation of protoplasts from an established *Arabidopsis thaliana* cell suspension culture and infection with RNA of turnip yellow mosaic tymovirus: A simple and reliable method. *J. Virol. Methods* **86,** 85–94.

Scholthof, K. B. G., Scholthof, H. B., and Jackson, A. O. (1995). The tomato bushy stunt virus replicase proteins are coordinately expressed and membrane associated. *Virology* **208,** 365–369.

Strauss, J. H., and Strauss, E. G. (1994). The alphaviruses: Gene expression, replication, and evolution. *Microbiol. Rev.* **58,** 491–562.

Ushiyama, R., and Matthews, R. E. F. (1970). The significance of chloroplast abnormalities associated with infection by turnip yellow mosaic virus. *Virology* **42,** 293–303.

van Pelt-Heerschap, H., Verbeek, H., Huisman, M. J., Loesch-Fries, L. S., and van Vloten-Doting, L. (1987). Non-structural proteins and RNAs of alfalfa mosaic virus synthesized in tobacco and cowpea protoplasts. *Virology* **161,** 190–197.

Watanabe, Y., Emori, Y., Ooshika, I., Meshi, T., Ohno, T., and Okada, Y. (1984). Synthesis of TMV-specific RNAs and proteins at the early stage of infection of tobacco protoplasts: Transient expression of the 30K protein and its mRNA. *Virology* **133,** 18–24.

Weiland, J. J., and Dreher, T. W. (1989). Infectious TYMV RNA from cloned cDNA: Effects *in vitro* and *in vivo* of point substitutions in the initiation codons of two extensively overlapping ORFs. *Nucleic Acids Res.* **17,** 4675–4687.

Weiland, J. J., and Dreher, T. W. (1993). *Cis*-preferential replication of the turnip yellow mosaic virus RNA genome. *Proc. Natl. Acad. Sci. USA* **90,** 6095–6099.